Earth and Planetary Science Letters, 68 (1984) 181–197
Elsevier Science Publishers B.V., Amsterdam – Printed in The Netherlands

[1]

The geochemical behavior of refractory noble metals and lithophile trace elements in refractory inclusions in carbonaceous chondrites

Bruce Fegley, Jr. [1] and Alan S. Kornacki [2,*]

[1] *Ceramics Processing Research Laboratory, Building 12-011, and Materials Processing Center, Massachusetts Institute of Technology, Cambridge, MA 02139 (U.S.A.)*

[2] *Smithsonian Astrophysical Observatory, 60 Garden Street, and Department of Geological Sciences, Harvard University, 24 Oxford Street, Cambridge, MA 02138 (U.S.A.)*

Received August 2, 1983
Revised version received February 14, 1984

Recent models of Ca, Al-rich inclusion (CAI) petrogenesis suggest that refractory inclusions may be residues of interstellar dust aggregates that were incompletely evaporated and partially melted in the solar nebula. These models, and the recent availability of new thermodynamic data, have led us to re-examine the traditional interpretation that lithophile refractory trace elements (LRTE) condensed as oxides in solid solution in refractory major condensates, while refractory noble metals (RNM) condensed as micron-sized nuggets of Pt-metal alloys. Calculations of LRTE-RNM alloy stability fields under nebular oxygen fugacities and partitioning experiments lead us to conclude that: (1) Ti, Zr, Nb, Hf, U, and Ta form stable alloys with RNM under nebular conditions; (2) the observation that metallic Zr, Nb, and Ta occur in some Pt-metal nuggets and grains is explained by the stability of these LRTE-RNM alloys under normal nebular oxygen fugacities; (3) metallic Ti, Hf, and U may also occur in some nuggets; (4) the lanthanides, the other actinides (Th, Pu), and Y do not form stable alloys, and thus probably do not occur alloyed with RNM; and (5) the partitioning of U (but not Th, Pu, or the REE) into RNM is a novel actinide and REE/actinide fractionation mechanism that is based on metal/silicate fractionation (rather than on the relative volatility of their oxides).

We propose that micron-sized Pt-metal nuggets formed from smaller grains of RNM alloys and compounds during the evaporation and melting of primitive dust aggregates. This process would have been enhanced by: (1) the possibility that the RNM were present as compounds (especially with As and S) as well as metallic alloys in interstellar dust and in some primitive meteoritical material, since they often exhibit non-siderophile behavior; and (2) the fluxing of volatiles through CAI's during distillation. Microscopic nuggets are common in melilite chondrules, indicating that residence in a slowly-cooled silicate melt may have favored their formation. Cation diffusivity and variations in local f_{O_2} can explain why metallic LRTE-bearing nuggets are not common in CAI's (despite the relative stability of LRTE-RNM alloys). We propose that the lithophile component of Fremdlinge is enriched in super-refractory elements, and that Group II CAI's formed from Fremdlinge-poor dust. We interpret the Group II REE fractionation as a pre-solar event, and predict that Nd/Sm dating will yield an age greater than the canonical age of the solar system. If metal/silicate fractionation in a cold solar nebula can explain Group II REE patterns, the possibility that Group II CAI's are also distillation residues cannot be excluded.

1. Introduction

Wänke et al. [1] first demonstrated that many siderophile and lithophile elements are fairly uniformly enriched to ~ 20 × chondritic levels in the Allende Group I [2] Ca, Al-rich inclusions (CAI's). Since all of these elements are refractory under equilibrium conditions with a gas of solar composition, the observed enrichments provide strong evidence that the minerals in these inclusions formed at high temperatures from a system that at

* Current address: Shell Oil Company, Western E and P Operations, Pacific Frontier Division (Woodcreek), P.O. Box 527, Houston, TX 77001, U.S.A.

0012-821X/84/$03.00

least approached chemical equilibrium with such a gaseous reservoir. Subsequently, Palme and Wlotzka [3], El Goresy et al. [4] and Wark and Lovering [26] discovered that siderophile refractory trace elements are concentrated in tiny metal nuggets and in complex aggregates of metal grains, some of which also contain metallic lithophile refractory trace elements (LRTE). These metal nuggets and grains have been interpreted as highly refractory condensates [3,4].

Certain LRTE (e.g., REE) are strongly fractionated in Group II CAI's [5]; siderophile refractory trace elements are also depleted in these objects [2]. Calculations by Boynton [6] first suggested that Group II REE patterns could have been produced by a two-stage condensation process in which the most refractory REE (Er, Lu) condensed from nebular vapor before formation of the Group II inclusions, which were then isolated from nebular gas before the most volatile REE (Eu, Yb) completely condensed. The interpretation that LRTE fractionations in Group II inclusions occurred during vapor-solid condensation at chemical equilibrium in hot gas of solar composition is compatible with the interpretation that CAI's are aggregates of refractory crystalline condensates [7].

However, models of CAI petrogenesis have become increasingly complex. Many CAI's appear to have experienced at least partial melting at some point [8]; Mason and Taylor [2] now characterize many Group I and Group V CAI's as Ca, Al-rich chondrules. Several authors [9,10 and references therein] have suggested that CAI's formed during the evaporation and melting of primitive dust aggregates, but because they are depleted in the most *refractory* trace elements, Group II inclusions cannot be refractory residues of unfractionated primitive dust. Wood [9] has suggested that Group II CAI's could have distilled from interstellar dust aggregates that had already been depleted in the super-refractory elements (SRE) by the physical fractionation of (unspecified) pre-solar trace phases enriched in SRE.

These new models of CAI petrogenesis, and the recent availability of new thermodynamic data, lead us to re-examine the geochemical behavior of the refractory noble metals (RNM) and several LRTE in CAI's in the context of distillation models. We review pertinent chemical and mineralogical properties of the various classes of refractory inclusions and present new calculations of the stability fields of LRTE-RNM alloys and several LRTE oxides under nebular conditions. These calculations, observational data, and experimental results are applied to a new model of the origin of refractory metal nuggets proposed independently by Kornacki and Cohen [11] and Cameron and Fegley [12]. Finally, we identify a specific mechanism for producing Group II *chemical* patterns in a cold solar nebula by fractionating interstellar dust at low temperature on the basis of *physical* differences between different populations of presolar grains, and discuss some implications of this model.

2. Mineralogical and chemical properties of refractory inclusions

Broadly speaking, there are two mineralogical classes (melilite-rich and spinel-rich) and two equivalent chemical classes (unfractionated and fractionated) of refractory inclusions in C3 chondrites. Characteristically, melilite-rich inclusions are relatively coarse-grained and fairly uniformly enriched in refractory elements. They have relatively flat Group I, III, V or VI or REE patterns (in which only the most volatile REE are fractionated) [2]. Spinel-rich refractory inclusions are usually fine-grained and relatively depleted in some refractory elements, with highly fractionated Group II REE patterns [5,13].

Refractory inclusions in C2 chondrites generally occur as small spinel-hibonite objects, although other inclusion types such as melilite-rich and hibonite-rich inclusions and fragments are also observed [14,15]. The most common refractory inclusions are spinel-perovskite or spinel-hibonite-perovskite spherules that some researchers consider to be igneous [15]. Irregular spinel-rich inclusions have also been described [14,15]. Refractory trace elements are usually more fractionated in C2 refractory inclusions that they are in melilite-rich, Group I Allende inclusions [16].

Several "ultra"-refractory inclusions that have

SRE fractionations *complementary* to those in Group II inclusions have also been identified in C2 and C3 chondrites [17–20].

2.1. Group I, III, V, and VI CAI's (unfractionated inclusions)

The LRTE (transition metals, lanthanides, and actinides) occur in major, minor, and trace oxide and silicate phases in Group I and Group V CAI's [21,22]. The RNM (Re, Ru, Os, Rh, Ir, Pt) are concentrated in two different trace phases: (1) rounded Pt-metal nuggets, and (2) Fremdlinge. Fremdlinge are complex objects whose origin remains enigmatic: they are "fluffy", multiphase aggregates of tiny metal, sulfide, oxide, phosphate, and silicate grains enriched in LRTE, siderophile refractory trace elements and many volatile elements [4]. The siderophile refractory trace elements occur in tiny metal grains with non-cosmic abundance ratios. The actinides (U, Pu, Th) occur with other LRTE (e.g. Sc, Zr, Y, Nb, Ta, REE) in non-metallic phases, including baddeleyite, perovskite, pyrochlore, and a new Ca-silicate with an apatite-like structure [23]. In addition, some Pt-metal grains in Fremdlinge contain metallic Nb and Ta [17,24].

Pt-metal nuggets are small (usually $\leqslant 3$ μm) metallic beads that contain RNM, Mo and W (two additional siderophile refractory trace elements), and Fe and Ni in various proportions [3,4]. The nuggets are extremely fine-grained intergrowths of several phases, since the siderophile refractory trace elements tend to segregate into distinct alloy phases on the basis of metallic crystal structures [25]. Wark and Lovering [26] report that Pt-metal nuggets in Type A CAI's contain RNM in roughly chondritic proportions; El Goresy et al. [4] report similar findings for nuggets in Type B CAI's. Fuchs and Blander [25], however, describe nuggets containing RNM in non-cosmic abundance ratios. Metallic LRTE (Zr, Cr, Nb, Ta) occur in some Pt-metal nuggets [4].

Since only a few Group III and Group VI CAI's have been identified, petrochemical data are limited. Refractory trace element data suggest that most Group VI CAI's are closely related to Ca, Al-rich chondrules (Group I and Group V CAI's).

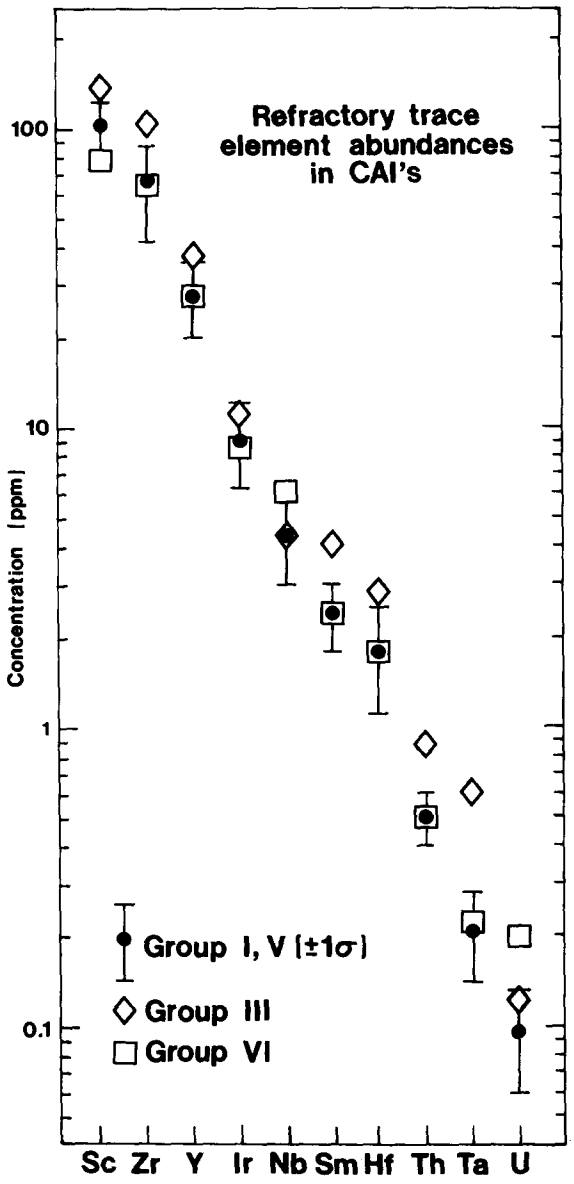

Fig. 1. Refractory trace element abundances in CAI's (excluding Group II). For most elements, abundances in Group VI CAI's are indistinguishable from those in Ca, Al-rich chondrules (Group I, V CAI's); most of these elements are more enriched in Group III CAI's. Element abundances in Group I, V CAI's based on 5 (Ta) to 37 (Sm) analyses reported by [1,2,5,7,21,27,28]; Group VI abundances are averages of 1 (Sc, Ta) to 6 (Zr, Hf, Sm) analyses reported by [2,5,21,28]; Group III abundances are averages of 2 (Ta) to 10 (Sm) analyses reported by [1,2,5,7,21,27,28].

The absolute abundances of Zr, Y, Ir, Sm, Hf, Th, and Ta in Group VI CAI's are indistinguishable from those in Group I and Group V Ca, Al-rich chondrules. In contrast, most refractory trace elements are more enriched in Group III CAI's (Fig. 1).

2.2. Group II CAI's (fractionated inclusions)

Group II inclusions are depleted in RNM and several LRTE (e.g., Er, Lu, Sc, Zr, Y, Hf) relative to the light REE [5]. Except for a single Pt, Ru-rich metal grain in the FUN inclusion EK 1-4-1 identified by Wark and Wasserburg [29], RNM-rich phases have not been reported in Group II inclusions. This is expected, since RNM are present in most Group II CAI's in only ~ chondritic abundances, or less [2,13]. The depletion of RNM in Group II inclusions (relative to other CAI's) could have been caused by the failure of trace phases (e.g., Pt-metal nuggets or grains) to accrete into these inclusions when they formed [30].

2.3. C2 inclusions

Inclusions in C2 chondrites are generally more refractory than those in C3 chondrites. Highly refractory minerals such as hibonite and corundum occur [15], and refractory trace elements often exceed the ~ 20 × enrichment characteristic of Group I Allende inclusions; e.g., LRTE (Sc, Ta, Th, Hf) and RNM (Ir, Ru, Os) are enriched to > 30 × chondritic levels in BB-3 (a spinel-hibonite spherule) [16]. Although RNM are more enriched in C2 inclusions than in Allende inclusions, Pt-metal nuggets and Fremdlinge are uncommon in them. The nearest analog is an Os, Ir-bearing troilite grain in OC-5, a botryoidal spinel-pyroxene aggregate described by MacPherson et al. [15].

2.4. "Ultra"-refractory inclusions

Six inclusions that are highly enriched in SRE have been identified in C2 and C3 chondrites. Their REE patterns resemble the hypothetical "lost" component that would account for Group II REE patterns [6].

Three ultra-refractory inclusions have been found in C2 chondrites. In SH-2 (a spinel-hibonite inclusion), there are large negative Eu and Yb anomalies, the heavy REE are enriched relative to the light REE, and the Os/Ru ratio is > 15 × chondritic [18]. The REE pattern of MH-115 (another spinel-hibonite inclusion) is similar; this inclusion also contains large amounts of Sc and Ir [19]. El Goresy et al. [20] inferred the presence of an ultra-refractory component in a refractory inclusion in the Essebi C2 chondrite. This ultra-refractory inclusion differs mineralogically from SH-2 and MH-115 (it contains melilite and fassaite in addition to spinel and hibonite), but one split has fractionated LRTE and siderophile refractory trace element patterns similar to theirs: the most refractory trace elements (e.g., Lu, Sc, Hf, Os, Re) are more enriched than less refractory ones.

Palme et al. [17] described one of the three ultra-refractory inclusions found in C3 chondrites. This tiny (~ 1 μg) inclusion from Ornans is greatly enriched in SRE: Lu and Hf are enriched to ~ 10^4 × their chondritic abundances; Re, Os, and Ir are enriched 1.5 × more than this. The Ornans inclusion contains a Fremdling that appears to be a mechanical mixture of Os-rich grains embedded in an Fe, Ni-rich matrix. Metallic Ta occurs in some of the Os-rich grains. Noonan et al. [31] described two glassy ultra-refractory inclusions (T-6 and T-7) in an Ornans amoeboid olivine aggregate. Zr-Y oxide crystallites and large heavy REE enrichments (> 10^4 × chondritic) occur in these objects.

3. The stability of LRTE-RNM alloys

Previous condensation calculations [7] predicted that LRTE such as Zr, Nb, and Ta condensed as oxides in the nebula, leaving unexplained the unusual geochemical affinity of *metallic* LRTE observed in some Pt-metal nuggets and Fremdlinge (e.g., El Goresy et al. [4] concluded that metallic LRTE-bearing nuggets are exotic objects that formed under extremely reducing conditions). In fact, this "puzzling" geochemical affinity can be explained by thermodynamic calculations, and is predicted by the Engel-Brewer correlation between

electronic configurations and phase stabilities of alloys [32].

Jones and Burnett [33], who experimentally measured Sm and actinide (U, Th, Pu) partitioning between silicate melt and metal, first noted the applicability of the Engel-Brewer correlation to the occurrence of metallic Zr in Pr-metal nuggets. Their experiments demonstrated that U (but not Th, Pu, or Sm) partitioned into Pt-metal at low oxygen fugacities ($\sim 10^{-22\pm3}$ atm) at $T \sim 1550$ K, on which basis they suggested that Zr-rich RNM nuggets may also contain U, and that partitioning into Pt-metals could cause fractionations among the actinides and between them and the REE in the solar nebula.

Fegley and Kornacki [30] independently used experimental and estimated thermodynamic data for several LRTE-RNM alloys to calculate their stability fields at nebular oxygen fugacities. These calculations are extended and revised in this paper; the results (plus other data on RNM alloys) are used in our discussion of the geochemistry of LRTE and RNM in refractory inclusions.

3.1. *Method of calculation*

Thermodynamic data from several sources were used: most data are from the JANAF tables and supplements [34] and Kubaschewski and Alcock [35]. Other sources used are cited in fig. 1 of

TABLE 1

Thermodynamic data for LRTE-RNM alloys [$\Delta G_f^\circ = A + BT$ (cal/mol)] (stable alloys italicized) *

Alloy	*A*	*B*	Alloy	*A*	*B*
$CeIr_2$ [a,b]	−38,100	3.0	$ThOs_2$	−38,360	11.9
$CePt_2$ [a,c]	−46,950	2.3	Th_3Os_2	−80,067	33.5
			Th_7Os_3	−149,379	63.8
$ErIr_2$ [a,c]	−36,400	2.3	$ThRh_2$	−70,500	9.0
ErPt [a,b]	−37,000	2.0	$ThRh_3$	−80,000	11.6
			$ThRh_5$	−80,400	12.0
$HfIr_3$ [a,d,e]	−78,100	9.6	ThRu	−30,600	7.3
$HfPt_3$	*−113,600*	*12.50*	$ThRu_2$	−35,610	9.72
$HfRh_3$ [a,f]	−77,600	12.0	Th_3Ru	−67,250	12.25
$NbIr_3$ [a,d]	*−49,000*	*9.6*	UIr_2	−52,400	0.2
$NbPt_3$ [a,d]	*−46,400*	*9.6*	*UIr_3*	*−60,000*	*−1.4*
			UOs_2	−42,800	9.7
$PuRu_2$ [a,c]	−22,100	2.3	*URh_3*	*−75,614*	*2.21*
$TaIr_3$	*−42,000*	*4.0*	URu_3	−42,673	3.89
$TaPt_2$	*−43,900*	*−2.73*	YIr_2	−36,400	2.3
$TaPt_3$	*−46,400*	*−7.64*	YPt [a,c]	−36,300	1.5
$TaRe_{3,6}$ [a,b]	*−33,100*	*4.6*	YRe_2	−32,460	1.8
$TiIr_3$ [b]	*−64,000*	*4.0*	*$ZrIr_3$*	*−86,800*	*12.8*
$TiPt_3$	*−81,700*	*8.01*	*$ZrPt_3$*	*−108,120*	*12.60*
$TiPt_8$	*−90,440*	*12.83*	*$ZrPt_5$*	*−110,700*	*13.86*
			$ZrRh_3$ [a,b]	−51,400	4.0
$ThIr_2$ [a,c]	−34,560	2.3	ZrRu [a,b]	−46,140	2.0
$ThIr_5$	−84,895	10.8	$ZrRu_2$ [a,b]	−55,560	7.2

* A complete listing of the thermodynamic data sources used is available from the senior author.

[a] Lower limit to ΔG_f° from the elements in Brewer and Wengert [32]; the actual ΔG_f° may be more negative.

[b] $\Delta S_f^\circ = -1.0$ cal/g-atom K assumed.

[c] $\Delta S_f^\circ = -0.76$ cal/g-atom K assumed by analogy with experimental data for UMe_3 alloys (Me = Rh, Ru).

[d] $\Delta S_f^\circ = -2.4$ cal/g-atom K assumed by analogy with experimental data for $MePt_3$ (Me = Ti, Zr, Hf), $TiPt_8$, and $ZrPt_5$ alloys.

[e] ΔG_f° also estimated using estimated thermal functions.

Fegley and Kornacki [30]. (Since our calculations are not condensation calculations, they are not dependent on elemental abundances).

The Gibbs free energy equations and stabilities of the RNM alloys are listed in Table 1. Complete thermodynamic data (i.e., experimentally measured thermal functions, ΔH_f° values from calorimetry, and ΔG_f° values from solid-state EMF measurements) are available only for URh_3 and URu_3. All other data include linear extrapolations of experimentally-measured Gibbs energy equations, and estimated thermodynamic properties; the details of these estimates are explained below.

Brewer and Wengert [32] give Gibbs free energy values (or their limits) for many RNM alloys of Zr, Hf, Nb, Ta, Ce, Er, Th, U, and Pu; these values were combined with estimates of the ΔS_f° values for alloy formation to yield linear Gibbs free energy equations of the form shown in Table 1. (A detailed description of the thermodynamic data evaluation is available from the senior author.) Several standard methods were used to estimate the entropy values. Kubaschewski and Alcock [35] recommend ΔS_f° values of ~ 0 cal/g-atom K for the formation of ordered alloys; Brewer and Wengert [32] estimate values of ~ -1 cal/g-atom K. The ΔS_f° values from solid-state EMF measurements of URh_3 and URu_3 yield an average value of -0.76 cal/g-atom K; ΔS_f° values from similar measurements of Ti, Zr, and Hf platinides give an average value of -2.4 cal/g-atom K. In some cases, several Gibbs free energy equations based on different estimated ΔS_f° values were calculated for the same alloys (e.g. $HfIr_3$, $NbIr_3$). The resulting f_{O_2} vs. $1/T$ lines were very close, demonstrating that the Gibbs free energy equations are relatively insensitive to the estimated ΔS_f° values. This is important, because it means that the results are not significantly affected by even relatively large changes in the thermodynamic data.

Selected estimates of Gibbs free energy equations were checked by making independent estimates using a different procedure. In this case, the Gibbs free energy values in Brewer and Wengert [32] were used again, but instead of making a Second Law estimate (i.e., assuming ΔH_f° to be constant and estimating a value for ΔS_f°), a Third Law estimate was made (by estimating the heat capacity (C_p°) and entropy (S_{298}^0) for the alloy; e.g., $HfIr_3$, $HfPt_3$, $ZrIr_3$). C_p° (at $T = 298$ K) was estimated to be 6.2 cal/g-atom K (using the Dulong-Petit rule); the temperature variation of C_p° was estimated by assuming it to be linear, with C_p° at the melting point equal to 7.25 cal/g-atom K [35]. The S_{298}^0 values for the alloys were estimated by assuming $\Delta S_f^\circ \sim 0$ cal/g-atom K (as recommended by Kubaschewski and Alcock [35]. Finally, the Gibbs free energy functions for the elements in the alloys (which are also required for a Third Law estimate) were taken from standard compilations [34,35]. Good agreement was found between the Second and Third Law estimates; our results are not dependent on the estimation method used.

The stability fields of the LRTE-RNM alloys were calculated from reactions of the type:

$$LM_3(s) + O_2(g) \rightarrow LO_2(s) + 3\ M(s) \qquad (1)$$

where L represents a LRTE and M represents a RNM. The equilibrium constant (K) for equation (1) is given by:

$$K_1 = (a_M^3)(a_{LO_2})/(f_{O_2})(a_{LM_3}) \qquad (2)$$

where a_i and f_j represent the activity of species i and fugacity of species j, respectively. When the oxygen fugacity is high enough to begin oxidizing the LRTE-RNM alloy, the three pure solid phases LM_3, LO_2, and M coexist at unit activity and the expression for K becomes:

$$K_1 = 1/f_{O_2} \qquad (3)$$

which defines a line in f_{O_2} vs. $1/T$ space. The LM_3 alloy is stable below this line (at lower oxygen fugacities); the LO_2 oxide is stable above this line (at higher oxygen fugacities); and LM_3, LO_2, and the metal M coexist on the line (at the equilibrium oxygen fugacity).

The LRTE oxides used in the calculations of the LM_3 alloy stability fields are those predicted to condense in the solar nebula. The oxides considered, the condensation temperatures of the *pure* oxides at $p = 10^{-3}$ bar, and the sources of the calculations are listed in Table 2. The effects of solid solution and compound formation (i.e., oxide components having less than unit activity) on the results of these calculations are discussed in section 4.3.

TABLE 2

Oxide condensation temperatures

Oxide	Condensation temperature (K)
ZrO_2	1825 [a]
HfO_2	1773 [a]
Y_2O_3	1692 [b]
TiO_2	1606 [c]
Er_2O_3	1590 [d]
ThO_2	1555 [e]
Ce_2O_3	1312 [d]
NbO_2	1309 [a]
Ta_2O_5	1306 [a]
UO_2	~1300 [e]
PuO_2	~1200 [e]

[a] This work.
[b] Boynton [6].
[c] $CaTiO_3$ condenses at 1677 K.
[d] Grossman and Ganapathy [21].
[e] Ganapathy and Grossman [36].

3.2. *LRTE-RNM alloy stability fields*

The calculated equilibrium f_{O_2} lines for important alloy stability fields are shown in Fig. 2. The LRTE-RNM alloy stability fields (solid lines) are superimposed on the solar nebula f_{O_2} at $p = 10^{-3}$ bar; the latter line was calculated from the H_2O and H_2 fugacities in the solar nebula, and is very insensitive to large changes in the total pressure.

Several important results that are demonstrated in Fig. 2 were briefly discussed by Fegley and Kornacki [30]. First, several alloys of Group IVB (Ti, Zr, Hf) and Group VB (Nb, Ta) elements with RNM are stable at nebular oxygen fugacities. We explain the occurrence of metallic Zr, Nb, and Ta in Pt-metal grains and nuggets as a consequence of the extraordinary stability of alloys of these LRTE with the RNM (the stability of Zr-RNM alloys is further illustrated in Table 3; these activity coefficients demonstrate that solutions of Zr in several RNM are highly non-ideal and highly favorable thermodynamically). We also note that it is not necessary to postulate highly reducing conditions (i.e., more reducing than nebular f_{O_2} values, including those under which the enstatite chondrites formed) to account for their formation.

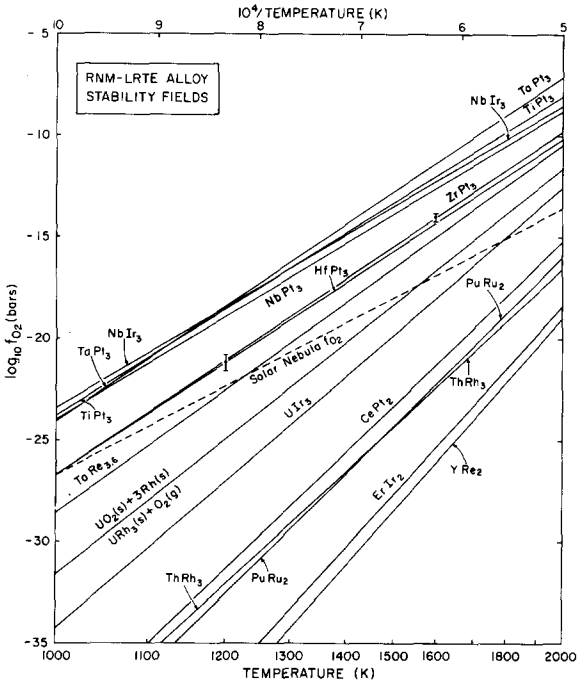

Fig. 2. Selected RNM-LRTE alloy stability fields (all alloys studied are listed in Table 1). Alloys with stability fields below the nebular f_{O_2} line (dashed) are unstable in the solar nebula; alloys with stability fields above this line are stable. Several alloys cross the nebular f_{O_2} line and become unstable at lower temperatures. Uncertainties in the thermodynamic data are reflected as uncertainties in the position of the alloy stability field. The uncertainty for alloys ($ZrPt_3$ and $HfPt_3$) with available experimental Gibbs free energy data are shown by error bars. Uncertainties in the estimated data are more difficult to assess, but at $T = 1400$ K an uncertainty of ± 5 kcal/mol (which is probably an overestimate) corresponds to ± 0.8 $\log_{10} f_{O_2}$ units. (Alloy stability fields are extended to 2000 K in order to illustrate trends. However, many alloys, metals, and oxides are not stable above 1600 K in the solar nebula.)

TABLE 3

Zr activity coefficients (γ) in RNM [32] ($\log_{10}\gamma$ at infinite dilution)

RNM	$\log_{10}\gamma$
Ru	−3.4
Rh	< −7
Ir	< −7
Pt	< −12

The second important result of our calculations is the conclusion that metallic Hf and Ti may also occur in some Pt-metal nuggets, although we believe that the geochemical behavior of a relatively abundant element such as Ti may be different than the behavior of trace elements such as Zr, Nb, Hf, and Ta (as discussed in section 4.3).

The third important result demonstrated in Fig. 2 is that RNM alloys of U, but not those of the other actinides (Th and Pu), are stable at nebular oxygen fugacities at very high temperatures. We conclude that metallic U may also occur in some Pt-metal nuggets. The formation of stable U-RNM alloys (but not Th- or Pu-RNM alloys) is a potential mechanism for actinide fractionation that is based on fractionating metallic and non-metallic carriers, rather than on the basis of the relative volatility of actinide oxides during condensation [37]. On the basis of their partitioning experiments, Jones and Burnett [33], independently suggested that Zr-bearing Pt-metal nuggets may also contain metallic U, and that the partitioning of U into Pt could cause actinide fractionation. However, D.A. Wark (personal communication, also cited in [33]) unsuccessfully searched for U in several Pt-metal nuggets (to concentrations of < 10 ppm) by fission track methods.

Finally, the fourth important result illustrated in Fig. 2 is that Y- and REE-RNM alloys are not stable at nebular oxygen fugacities. Thus, we conclude that metallic Y and REE are probably absent from Pt-metal grains and nuggets. This conclusion is in accord with the experimental results of Jones and Burnett [33], who observed no Sm partitioning into Pt. They independently suggested that the partitioning of U (but not Sm) into Pt is a mechanism for actinide/REE fractionation in the solar nebula.

4. Discussion

4.1. Condensation in a hot solar nebula

Two important assumptions of equilibrium condensation models are that: (1) the solar nebula was hot enough to vaporize all presolar dust; and (2) thermodynamic equilibrium was maintained between low pressure ($\leqslant 10^{-3}$ bar) nebular gas and crystalline condensates from it [7]. The first assumption is in conflict with the observed preservation of extrasolar isotopic anomalies in very volatile elements (e.g., H, C, N, O, noble gases) and refractory elements (e.g., Ba, Ca, Nd, Sm, Sr, Ti), which strongly suggest that presolar dust was not completely vaporized in the solar nebula. For example, Wood [9] demonstrated why the occurrence of ubiquitous oxygen isotope anomalies preclude the complete vaporization of interstellar dust in the solar nebula. Recent astrophysical models also suggest that only a small volume of the solar nebula was sufficiently hot to completely vaporize all presolar dust [12].

The second assumption has been repeatedly tested theoretically [12] and experimentally [38]; both types of studies show that amorphous, non-stoichiometric materials nucleate under nebular conditions, but not until the gas has become greatly supersaturated by cooling significantly below the equilibrium condensation temperature. Since it is probably more difficult under nebular conditions to nucleate micron-sized phases enriched in trace metals (like the RNM) than major silicate and oxide phases, the interpretation that Pt-metal nuggets are nebular condensates depends partly on the demonstration that silicate and oxide condensates occur in CAI's. In fact, the inferred crystallization sequences (hibonite → spinel and spinel → melilite) between the two most abundant minerals in spinel-rich and melilite-rich inclusions contradict the condensation sequence. The observed crystallization sequences probably result from such processes as partial melting or sintering of more primitive material [8,10,39]. The condensation model also fails to explain the low Ca/Al ratios [5] (manifested by the absence of melilite, an important condensate), and the absence of calcium dialuminate (a condensate that is stable over a large *P-T* range in the solar nebula [40] in spinel-rich refractory inclusions.

If microscopic Pt-metal nuggets are primitive condensates, it is reasonable to expect that nuggets would occasionally be found in meteoritical constituents (other than CAI's) that are also interpreted to be relatively primitive nebular material. This is especially true for enstatite chondrites, and

meteorite matrix in CV3 and unequilibrated ordinary chondrites, all of which probably contain primitive nebular material in abundance, and which may even be aggregates of condensates. But Pt-metal nuggets have not been observed in any of these materials. It is especially significant that, except for a RNM-bearing troilite grain in a spinel-pyroxene aggregate [15], Pt-metal nuggets have not been observed in C2 refractory inclusions that are richer in RNM than are nugget-bearing Allende CAI's. Cameron and Fegley [12] also emphasized this: they noted that although the RNM condense at a higher temperature than the oxide minerals found in C2 refractory inclusions (e.g., at $p = 10^{-5}$ bar, Os condenses at 1747 K while hibonite and spinel condense at 1548 and 1337 K, respectively [40]), Pt-metal nuggets are not found in these CAI's, except in an inclusion in Essebi [20] which may have been partially molten. This observation is compatible with out proposal that micron-sized Pt-metal nuggets form by the consolidation of many smaller submicroscopic metal grains while immersed in a silicate melt (see section 4.2).

4.2. Evaporation and melting of interstellar dust aggregates

Several properties of CAI's that are inconsistent with condensation models can be explained if CAI's formed during the evaporation and melting of interstellar dust aggregates. Wood [9] explained how oxygen isotope data support this model for CAI petrogenesis. Most CAI's are not simply porous aggregates of crystals: many Group I, V and (perhaps) VI CAI's are Ca, Al-rich chondrules [2]; "fluffy" Type A CAI's are welded aggregates of smaller rimmed objects [41]; fine-grained (Group II) CAI's are complex aggregates of tiny rounded, rimmed, spinel-rich bodies that may be igneous objects [10,39]. Partial melting at moderately high temperatures ($\sim$ 1700 K), and crystal/liquid fractionation by splashing, ablation, or evaporation explains the Ca/Al fractionation observed in bulk analyses of spinel-rich CAI's [2] and in their mineralogical constituents [10].

The geochemical behavior of RNM and LRTE in CAI's should be re-examined in the context of evaporation and melting models, especially since distillation models explain the important bulk RNM and REE fractionations observed in Group I, III, V and VI CAI's (in which the refractory trace elements are relatively unfractionated or only the most volatile RNM and REE are fractionated) as well as condensation models. If thermodynamic equilibrium were maintained, it would be difficult to distinguish between the effects of condensation and distillation (since in principle the processes are the inverse of each other). But kinetic factors are also important in geochemical processes, and we note an important difference between condensation and distillation applicable to the evolution of CAI's: the formation of micron-sized phases enriched in trace elements (e.g., LRTE, RNM) is less problematical in the case of distilling primitive dust aggregates since the trace elements are already "pre-condensed" (in submicroscopic grains), nucleation constraints are less severe, diffusion/devolatilization rates come into play, and the fluxing of volatile species would likely catalyze solid $\rightarrow$ solid reactions (of the type illustrated in Fig. 2) by the formation of intermediate compounds. Trace element patterns in Group II inclusions, which are an exception, will be discussed in section 4.4.

If CAI's formed by melting and evaporation of primitive dust aggregates, microscopic Pt-metal nuggets could have formed by the consolidation of sub-microscopic, RNM-rich grains during distillation. Jovanovic and Reed [42] concluded that submicroscopic Pt-metal grains are abundant in coarse-grained CAI's and in Allende meteorite matrix. The nucleation constraints against condensing *micron*-sized trace element nuggets with chondritic abundance ratios from nebular vapor would not apply if the RNM were already present in the condensed state in sub-microscopic, pre-solar dust. The RNM might have originally condensed with fractionated abundances into primitive dust grains (fractionated RNM patterns have been measured in the tiny metal grains that comprise Fremdlinge [4]), but an aggregate of primitive dust would probably sample enough fractionated metal grains to restore chondritic ratios to the bulk sample. RNM condensation could have occurred in stellar envelopes or in the interstellar medium. (Wood [9]

TABLE 4

LRTE and RNM abundances

	(Si = 10^6)		
Zr	11	Ru	1.9
Nb	0.71	Pt	1.4
Hf	0.18	Os	0.72
U	0.024	Ir	0.66
Ta	0.023	Rh	0.34
		Re	0.05
			(Σ = 5.1)

Data from Anders and Ebihara [43].

reviewed evidence for dust condensation in these two environments.)

The RNM are so enriched in large, Group I Ca,Al-rich chondrules that a large number of micron-sized Pt-metal nuggets would form by the consolidation of sub-microscopic RNM-rich grains during distillation. Group I CAI's typically contain ~ 30 wt.% SiO_2, and RNM are enriched ~ 15 × more than their chondritic abundance of 5.1 ppm (relative to Si; Table 4) [2]. A single 110-μm Pt-metal sphere would account for the entire inventory of RNM in a Group I CAI with a diameter of 5 mm. (These calculations are also based on a mean RNM gfw of ~ 170 g/mol and a mean RNM density of ~ 18 g/cm^3 (calculated from their relative chondritic abundances [43]), and a CAI density of ~ 3 g/cm^3.) But Pt-metal nuggets are usually much smaller than this [4,25], and it would require ~ 1.7×10^5 2-μm nuggets to account for the RNM in the CAI; their density on a thin section surface would be ~ 10 nuggets/mm^2. In BB-3 (a 170-μm-diameter spinel-hibonite spherule in which RNM are enriched to ~ 30 × chondritic levels [16], however, the RNM inventory would be accounted for by only ~ 15 2-μm nuggets: the *absolute* abundance of RNM atoms is simply too low in this small spinel-hibonite chondrule to have formed many microscopic nuggets. This can explain why micron-sized Pt-metal nuggets have not been observed in C2 refractory inclusions, which are usually small objects ($\leq$ 200 μm), even though the relative abundance of RNM is ~ 2 × greater in them than in nugget-bearing C3 CAI's. Otherwise, if micron-sized Pt-metal nuggets (such as those found in Ca,Al-rich chondrules) are condensates that grew to that size during condensation from nebular gas and C2 inclusions are aggregates of condensates, we see no inherent reason why observable nuggets should be so uncommon in C2 inclusions.

We also suggest that some portion of alloy-forming LRTE that are supposedly dissolved as oxides in perovskite, spinel, hibonite, melilite, and other major CAI phases are actually *metals* alloyed with RNM in sub-microscopic Pt-metal inclusions in these minerals. Zr is too abundant to be completely condensed alloyed with RNM, but a significant amount of Nb, Hf, Ta, and U could reside in such alloys (Table 4).

The RNM are much too refractory to have melted at the temperatures (< 2000 K) at which interstellar dust aggregates were processed to form CAI's: their 1 atm melting points range from ~ 2050 K (Pt) to > 3300 K (Os) [44]. Some pure or nearly pure RNM grains have been reported; e.g., El Goresy et al. [4] described pure Ru grains and nearly pure Re grains (97 wt.% Re; 3 wt.% Ru). Most RNM grains are alloys with lower (unknown) melting points. But the Pt-group "noble" metals are more reactive than their name suggests. Although their strongest geochemical affinity is for metal alloys, they also have affinities (in order of decreasing intensity) for sulfarsenides, arsenides, sulfides, oxides, and silicates [44]. The Pt-group metals form many compounds with metallic, semi-metallic, and chalcophilic elements in Group IIIA (In, Tl), Group IVA (Sn, Pb), Group VA (P, As, Sb, Bi), and Group VIA (S, Se, Te) [44]. The principal terrestrial Pt mineral is sperrylite ($PtAs_2$); other important ore minerals include cooperite (PtS) and braggite ((Pt, Pd)S) [44]. Pd and Rh are soluble in pyrrhotite [44]. Chromite is an important concentrator of Pt-group metals in the Bushveld Igneous Complex. During fractional crystallization in the absence of sulfur/arsenic, Ir, Ru, and Os partition into ferromagnesian silicates (although it is uncertain whether the Pt-group metals occur as metallic inclusions or in solid solution in these oxides and silicates [44]. Pt also forms organic compounds with kerogen [44]; kerogen-like hydrocarbons

account for > 70% of the organic material in chondrites [45].

Although the mineralogical and geochemical behavior of the Pt-group metals in terrestrial environments can be applied to their behavior in astrophysical regimes only with caution, these observations suggest that the RNM probably had a very complex cosmochemical history. Subsequent to their nucleosynthesis and possible condensation as metal grains, they could have reacted at lower temperatures in extra-solar environments to form compounds with As, S, and other elements, or dissolved in solid solution (especially in sulfides). Thus, RNM may have been present in interstellar dust aggregates as compounds, as well as metallic alloys. This seems to explain the results of Jovanovic and Reed [42], who obtained RNM-enriched carbon-rich residues from acid-demineralized bulk samples of Allende. They noted that large fractions of Ru, Os, and Ir in bulk Allende and coarse-grained CAI's were soluble in ascorbic acid-hydrogen peroxide or HCl-HF, and concluded that most of the Pt-group metals occur in sulfides, FeNi metal, silicates, or oxides (since RNM alloys would be impervious to these acids).

Two processes would have promoted the formation of Pt-metal nuggets from oxidized RNM-rich phases during the evaporation and melting of interstellar dust aggregates. First, RNM compounds have much lower melting temperatures than metallic alloys or pure elements: e.g., the Pt-As eutectic occurs at 870 K, and RuS melts at ~ 1400 K [44]. Immiscible RNM-bearing droplets that formed at moderately high temperatures could have grown into larger molten objects, especially if they were immersed for hours or longer in a semi-molten proto-CAI. At even higher temperatures, volatile elements like As and S would have evaporated, leaving a microscopic metallic bead as a refractory residue.

The second process, analogous to fire assaying in the presence of fluxes (an important metallurgical extractive technique), would have supplemented the first one. Pt-group metals are assayed from their ores by fluxing them with Na_2CO_3, K_2CO_3, CaF_2, $Na_2B_4O_7$, and SiO_2 in the presence of metallic collectors (e.g., Pb, Ag, Cu, Sn, Cu-Ni sulfides). Fusing is done on time scales and at temperatures reasonable for CAI distillation: ~ 1200 K for 17 minutes, followed by ~ 1300 K for 15 minutes [44]. It is not known if the fluxes used by metallurgists occur in interstellar dust, but an analogous process could have occurred as ices and moderately volatile elements melted, evaporated, and fluxed through the proto-CAI as it was distilled. During either process (simple melting or fluxed fire-assaying), the chondritic Pt-metal ratios observed in some Pt-metal nuggets [4,26] could have been restored by the combining of many smaller, fractionated Pt-metal grains.

Both of these processes also could have redistributed the refractory trace metals Mo and W. Palme et al. [17] argued that the formation of volatile Mo and W oxides during evaporation processes ought to deplete CAI's in these elements. But metallic Mo and W could also form sulfides during melting and fluxing; MoS_2 and WS_2 occur in some RNM-rich aggregates [4,25]. Our unpublished calculations of RNM, Mo, and W sulfide stabilities show that MoS_2 and WS_2 can form at low sulfur fugacities ($f_{S_2} \sim 10^{-10.5}$ bar at 1000 K), while RNM sulfides require substantially higher ($\sim 10^{-3}$ to 10^{-7} bar at 1000 K) sulfur fugacities. If relatively volatile sulfides were originally present in primitive dust aggregates, their decomposition during distillation would provide the necessary sulfur fugacities for Mo and W sulfide formation. Thus, these two elements could be oxidized and redistributed (metal → sulfide) without being lost during the processing of proto-CAI material.

4.3. Constraints on the formation and abundance of LRTE-RNM alloys in the solar nebula

Although our results and the experimental work of Jones and Burnett [33] strongly indicate that metallic LRTE such as Zr, Nb, Hf, Ta, and U should be present in Pt-metal nuggets, metallic LRTE-bearing nuggets are not common. Furthermore, although Ti-RNM alloys are stable at nebular oxygen fugacities, metallic Ti has not been observed in Zr-, Nb-, and Ta-bearing nuggets. There are several factors which may be responsible for these apparent discrepancies between theory and observations.

First, the results presented in Table 1 and Fig. 2

will be altered if the LRTE are not present as pure oxides. For example, compound and solid-solution formation by the LRTE will reduce their oxide activities to less than unity; this will decrease the equilibrium f_{O_2} value for LRTE-RNM alloy formation. We illustrate the magnitude of this effect for the ZrO_2-$ZrPt_3$ equilibrium reaction.

Watson and Harrison [46] give data on zircon saturation in crustal magmas for the reaction:

$$ZrO_2(\text{magma}) + SiO_2(\text{magma}) = ZrSiO_4(s) \quad (4)$$

The equilibrium constant for reaction (4) can be calculated from the JANAF tables [34]. From the published concentrations of Zr and SiO_2 in the melt at zircon saturation [46], activity coefficients of $\sim 10^2$–10^3 are estimated for ZrO_2 at concentrations of several hundred to a few thousand ppm Zr. (An additional assumption is ideal solution of SiO_2 in the melt. The extensive data of Rein and Chipman [47] for SiO_2 activities in ternary and quaternary melts in the CaO-MgO-Al_2O_3-SiO_2 system show that SiO_2 activity coefficients are ~ 1 for the compositions studied by Watson and Harrison [46]. Thus, the assumption of ideality for SiO_2 is reasonable.)

For a ZrO_2 concentration of ~ 90 ppm (which is typical of Type B Allende CAI's [1] and a ZrO_2 activity coefficient of $10^{2.5}$, the equilibrium f_{O_2} value required for $ZrPt_3$ stability at 1500 K (calculated from equation (1) is $10^{-17.0}$ bar, which is slightly lower than the f_{O_2} value of $10^{-15.4}$ bar calculated assuming unit activities for ZrO_2 and Pt but higher than the solar nebula f_{O_2} (value ($10^{-18.0}$ bar) at the same temperature.

The additional effect of Pt solid solution in Pt-metal nuggets on the $ZrPt_3$ stability field also can be evaluated by assuming ideal solid solution of Pt in the RNM alloy [3,17]. Again, using a ZrO_2 concentration of 90 ppm and an activity coefficient of $10^{2.5}$, and a Pt concentration of ~ 10 wt.% (which is appropriate for alloys formed at ~ 1500 K [3]), the equilibrium f_{O_2} value for $ZrPt_3$ stability is lowered to $10^{-21.7}$ bar. But the higher Pt concentrations in nuggets (~ 83 wt.%) reported by Wark [48] require f_{O_2} values of only $\sim 10^{-17.3}$ bar. El Goresy et al. [4] and Fuchs and Blander [25] have also described Pt-rich alloys and nuggets containing as much as 60 wt.% Pt.

These calculations indicate the extent to which a representative alloy stability field is changed by LRTE and RNM solid solution. But because the chemical form of LRTE and RNM in interstellar dust grains is unknown, it is difficult to establish definitive constraints on the formation of specific LRTE-RNM alloys. For example, although Zr and Nb are present only as trace elements in bulk inclusions, pure phases such as ZrO_2 and $Ca_2Nb_2O_7$ occur in CAI's [4,23]. Perovskites with high Zr and Nb contents also occur ([22] and A. El Goresy, personal communication). Calculations of the relative stabilities of Ti, Zr, Nb, Hf, and Ta carbides and nitrides vs. their respective RNM alloys show that metallic LRTE are also stable under reducing conditions applicable to the formation of enstatite chondrites in the solar nebula or dust in cool stellar atmospheres with high C/O ratios [49].

Second, our results apply to binary LRTE-RNM alloys, while Pt-metal nuggets are actually complex alloys of several RNM with Fe, Ni, and Mo [4,25]. A more realistic analysis of LRTE-RNM alloy formation should consider the stability of multi-component alloys of two or more RNM with LRTE, but the lack of any thermodynamic data for multicomponent LRTE-RNM alloys makes this investigation impossible at present.

A related problem is the almost complete absence of thermodynamic data for LRTE solid-solution in RNM. Brewer and Wengert [32] placed limits on the activity coefficient of Zr dissolved at infinite dilution in several RNM (Table 3). Meschter and Worrell [50] determined $\overline{\Delta G}_{Zr}$ in Pt at $X_{Zr} = 0.02$, which yields $\log_{10}\gamma_{Zr} = -14.6$ (at $T = 1300$ K), in agreement with the value given by Brewer and Wengert [32] of < -12. However, the temperature and concentration dependence of γ_{Zr} in Pt are not known, nor are we aware of any data for the activity coefficients of other LRTE's in Pt or any other RNM. If data were available for several binary systems (e.g., Zr-Pt, Pt-Ru, Zr-Ru), then estimates of γ_{Zr} in the Zr-Pt-Ru ternary could be made using formalisms such as the Redlich-Kister or Kohler equations; these estimates could then be used to estimate Zr concentrations in Pt-metal nuggets composed primarily of Pt and Ru. Unfortunately, this method cannot be ex-

tended easily to quaternary or higher systems, for which it is more desirable to employ interaction coefficients (parameters that allow a thermodynamic treatment of dilute multi-component solutions [35]). Again, this more sophisticated analysis requires data that are not currently available. Either of these treatments is desirable because they would allow semi-quantitative calculations of the amount of LRTE that can dissolve in Pt-metal nuggets under different conditions (which can help to constrain various formation scenarios).

Another factor that may account for the relative rarity of metallic LRTE-bearing Pt-metal nuggets is variations in f_{O_2} during or following nugget formation. Jones and Burnett [33] first mentioned this possibility to resolve the apparent contradiction between their experimental results (indicating U partitioning into Pt at low oxygen fugacities) and Wark's observations (showing no U in many Pt-metal nuggets). For example, it seems likely that a distilling proto-CAI would produce a local environment more oxidizing than that of the nebula. This would be a complicated process, depending on mixing rates between H_2-rich nebular gas and O-rich vapor produced by the dissociation of precondensed ices, oxides, and silicates. Davis et al. [51], examining a simple model for the hibonite-rich FUN inclusion HAL, demonstrated how this effect explains the unusual REE fractionations found in that CAI. Eu and Yb fractionations in Group III and Group VI CAI's and in unclassified inclusions [2,18] could also be due to this effect, since the volatility of these REE depends on their oxidation state [6]. The non-siderophile behavior of Ti, Zr, Nb, Hf, and Ta in most CAI's is explained if local oxygen fugacities usually exceeded nebular values by three or four orders of magnitude (Fig. 2).

In principle, several potential indicators of local oxygen fugacities exist in CAI's, including Ti^{3+}/Ti^{4+} ratios in fassaitic pyroxenes, the color of hibonite [52], Ce^{3+}/Ce^{4+} ratios in REE-bearing phases [51], co-existing oxide/sulfide minerals in Fremdlinge [4], and co-existing ferrous (e.g., olivine, pyroxene, spinel) and ferric (e.g., andradite) minerals. In practice, however, the use of these potential indicators is very complex. Some phases (such as fassaitic pyroxene) are probably primary minerals that crystallized from a melt [8]; other primary phases (such as hibonite) have probably been altered to various degrees [22,52]; andradite (which occurs in rims) may be entirely secondary; the origin of phases in Fremdlinge is uncertain. As a result, it is far from clear to what stage of the history of a CAI the f_{O_2} indicated by a particular system corresponds, and the use of these potential indicators is fraught with complications. Direct measurements of the intrinsic f_{O_2} vs. $1/T$ for different types of refractory inclusions and for their various constituents (i.e., mineral separates from the core and rims), would be very useful.

Finally, the apparent absence of Ti in Pt-metal nuggets may be due to the relative abundance of that element in refractory inclusions. Unlike the other alloy-forming LRTE (which are trace elements and do not usually form their own minerals), Ti is a major constituent of perovskite and fassaitic pyroxene (two common CAI minerals). During the evaporation of interstellar dust grains, cation diffusion through oxide and silicate mineral lattices is probably an important process for the formation of LRTE-RNM alloys. Ionic diffusion in oxides depends on several factors, such as the temperature, ambient atmosphere, the presence of impurities, and the existence of lattice defects and high diffusivity paths in the crystal structure. Cations such as tetravalent Zr, Hf, and U and pentavalent Nb and Ta may have larger diffusivities in an oxide lattice such as perovskite or pyroxene than does Ti^{4+} (especially since the Ti atoms are structural elements of the mineral lattices). This supposition is not unreasonable, considering data on cation diffusivity in rutile (TiO_2). Yan and Rhodes [53] found that small cations such as Al^{3+} (0.53 Å), Co^{3+} (0.61 Å), Ga^{3+} (0.62 Å), Mg^{2+} (0.72 Å), and Fe^{2+} (0.77 Å) rapidly diffuse through rutile by an interstitial diffusion mechanism. O'Bryan and Yan [54] found that Ba^{2+} (1.35 Å) also diffuses rapidly through rutile by lattice and surface diffusion, and that the diffusivities of Al^{3+}, Co^{3+}, Ba^{2+}, and Fe^{2+} are greater than the self-diffusivity of Ti^{4+} in rutile. The ionic radius of Ta^{5+} (0.68 Å) is equal to that of Ti^{4+} (0.68 Å), but those of tetravalent Nb (0.74 Å), Hf (0.78 Å), and Zr (0.79 Å) (which are approximately equal to the ionic radius of Fe^{2+}) and U (0.97 Å) are all

significantly larger. Thus, kinetic factors may contribute to the apparent absence of metallic Ti in Pt-metal nuggets.

4.4. SRE fractionations as a result of metal/silicate fractionation in a cold solar nebula

The occurrence of refractory inclusions depleted in SRE does *not* require fractionation of highly-refractory condensates in a hot solar nebula soon after the onset of condensation. It only requires the physical fractionation in the nebula of primitive dust with a "memory" of an earlier high-temperature history prior to the formation of Group II inclusions. Clayton [55] has long argued that many of the unusual isotopic and chemical features of refractory inclusions manifest the "chemical memory" of their pre-solar history.

We propose that the SRE-rich component complementary to Group II inclusions formed in a pre-solar environment. SRE-rich dust could have formed by condensation in a stellar atmosphere, where dust formation is known to occur (references cited in Wood [9]), or by chemical processing, such as sputtering, in the interstellar medium [56]. We also propose that the SRE-rich component is preserved in the form of Fremdlinge. In this model, SRE-rich oxide dust and RNM-rich grains accreted in Fremdlinge (or "proto"-Fremdlinge) prior to the formation of the solar nebula or during the early collapse stages of solar nebula formation [4]. Fremdlinge were later fractionated from metal-poor dust on the basis of differences in physical properties (such as density, magnetic susceptibility, or sticking factor). The resulting physical fractionation has the appearance of a high-temperature chemical fractionation in the nebula—with one important difference. If this process is responsible for the formation of SRE-poor Group II inclusions, then the REE fractionations in these inclusions will have presolar ages (as determined by the Nd-Sm dating technique). Evidence which we feel supports our model and further implications are discussed below.

The first stage of our model is the chemical fractionation of SRE (such as Er, Lu, Sc, Zr, Y, Hf) from less refractory elements. While other authors such as Boynton [6] have proposed that this high-temperature chemical fractionation occurred in the solar nebula, we propose that it occurred in a pre-solar environment. Unfortunately, the astrophysical constraints on dust formation in stellar envelopes and secondary processing (e.g., sputtering) in the interstellar medium are poorly understood. Thus, a quantitative description of presolar chemical fractionation is not possible. However, the only requirement of our model is that this fractionation occurred prior to solar nebula formation.

The second stage of our model, the accretion of SRE-rich and RNM-rich grains into Fremdlinge (or "proto"-Fremdlinge) could have occurred in an (unspecified) pre-solar environment or during the early stages of the collapse of the solar nebula. Two possible environments are stellar atmospheres and the interstellar medium. However, this model does not require the Fremdlinge in meteorites to be well-preserved aggregates of interstellar dust grains or unaltered condensates from supernova ejecta. Many Fremdlinge occur in Ca, Al-rich chondrules and we find it difficult to understand how "fluffy" aggregates of interstellar dust could have retained their textures once they were incorporated into molten objects. Fremdlinge are usually enclosed in Ti-Al-pyroxene and melilite (the CAI minerals most likely to have crystallized from a melt [8]), but only adhere to spinel (the mineral least likely to have been molten) [4,24]. This suggests that Fremdlinge were once bathed by molten material, and seems to support the interpretation of Wark and Lovering [26], although the metasomatism they propose should only have added volatiles to the final alteration assemblage.

The third stage of our model is the separation of Fremdlinge (or "proto"-Fremdlinge) from metal-poor dust on the basis of differences in their physical properties. This metal/silicate fractionation created reservoirs of Fremdlinge-rich and Fremdlinge-poor dust. Group II inclusions formed during the evaporation and melting of aggregates of Fremdlinge-depleted dust; ultra-refractory inclusions formed from the Fremdlinge-rich reservoir. Inclusions that display relatively uniform enrichment factors among refractory lithophile and siderophile elements, e.g., Group I CAI's [1], formed in a different region of the nebula (where

this fractionation did not occur), or formed before or after the fractionation, when dust was not separated or had been remixed. Alternatively, the Ca,Al-rich chondrules may be uniformly enriched in refractory elements because of their large size [39]. Large chondrules sampled a larger number of interstellar grains than did smaller inclusions, and grain-to-grain chemical variations were eliminated.

Our model requires that the SRE pattern of Fremdlinge be that of the component whose loss is responsible for Group II SRE depletions. In support of this idea, we note that the most ultra-refractory inclusion identified to date is a tiny (~ 1 μg) inclusion studied by Palme et al. [17]. We propose that Palme et al. [17] actually measured the trace element pattern of a large Fremdling. Unfortunately, the mineralogical nature of this ultra-refractory inclusion is unclear because after the trace element composition of the object was measured by INAA, a portion of the inclusion was lost in handling before Palme et al. [17] studied it petrographically by SEM microscopy: only an $\sim$ 10-μm fragment of a Type 2 Fremdling was preserved. (El Goresy et al. [4] identified three types of Fremdlinge, which are differentiated primarily on the basis of the relative abundance of FeNi-metal and the texture of their non-metallic component.) Since a spherical Type 2 Fremdling with a specific gravity of ~ 7.5 (Type 2 Fremdlinge contain ~ 80 vol.%. FeNi-metal ($\rho \sim 7.8$ g/cm^3), ~ 15 vol.% silicate/oxide grains ($\rho \sim 3$ g/cm^3), and 5 vol.% RNM grains ($\rho \sim 18$ g/cm^3)) and a diameter of 65 μm would have the required mass of ~ 1 μg, it is possible that this ultra-refractory "inclusion" was simply a very large Fremdling, or at least that the SRE-rich lithophile component of the preserved Fremdlinge (plus any material subsequently lost) contributed significantly to the measurements performed on the entire tiny inclusion.

5. Conclusion

We have proposed that micron-sized Pt-metal nuggets in CAI's (including those that contain metallic LRTE) formed from smaller grains of RNM alloys and compounds during the distillation and melting of interstellar dust aggregates, and that Group II fractionations are an expression of the "chemical memory" of pre-solar dust. Our model has three advantages. First, the correlation between LRTE and RNM fractionations observed in most Group II and ultra-refractory inclusions is explained by the fractionation of a single component (Fremdlinge). Second, it also explains why the RNM and Pd are depleted but *unfractionated* in Group II inclusions [2]; in all other chemical classes of CAI's, Pd is depleted relative to the RNM. If the reservoir from which Group II CAI's formed lost RNM at high temperatures, there must have been a second fractionation that coincidentally removed the same fraction of Pd. It is simpler to suppose that all of the Pt-group metals were lost in a single, low-temperature fractionation. (H. Palme, personal communication, warned that a metal grain from Allende meteorite matrix is sufficient to contaminate the Group II inclusions with Pd and RNM in the proportions reported by Mason and Taylor [2]. We strongly urge that RNM and Pd analyses of additional Group II inclusions be performed to confirm their results.) Finally, our model is independent of (but in harmony with) the chemical evidence that led Wark [57] to suggest an early fractionation of sulfides from silicates in a cold (< 700 K) solar nebula.

Our model also has several important implications. First, we propose that REE fractionations in Group II material occurred in an (unspecified) pre-solar environment, and predict that Nd-Sm dating of Group II inclusions will yield pre-solar ages. Second, if the physical fractionation of Fremdlinge-rich and Fremdlinge-poor dust was widespread spatially or temporally, Group II inclusions ought to be a significant fraction of refractory inclusions. Third, our calculations of LRTE-RNM alloy stabilities demonstrate that Ti, Zr, Hf, Nb, Ta, and U can exhibit siderophile affinities under redox conditions applicable to the solar nebula (and perhaps some planetary interiors such as the parent body of the enstatite chondrites). This unanticipated behavior of elements that are usually considered to be lithophile could have important geochemical consequences, especially for planetary heat production and thermal evolution (if U partitions into planetary cores) and geochro-

nology: siderophile behavior of Hf could have important implications for the proposed ^{182}Hf chronometer for the early solar system [58].

Acknowledgements

This research was supported by NASA grants NGR 22-009-521 to J.S. Lewis, NGL 22-007-269 to A.G.W. Cameron, NGL 09-015-150 to J.A. Wood, and NSF grant Atm 81-12341 to R.G. Prinn. The senior author also appreciates support from H.K. Bowen and R.L. Pober at the cosmoceramics division of the CPRL, MIT. Discussions with L. Brewer, J.A. Wood, D.A. Wark, A. El Goresy, H. Palme, J.H. Jones, A.G.W. Cameron, and R.E. Cohen were especially enlightening. The clarity of this paper was improved through the editorial efforts of K. Motylewski, and by thoughtful reviews by H. Palme and two anonymous referees.

References

1 H. Wänke, H. Baddenhausen, H. Palme and B. Spettel, On the chemistry of the Allende inclusions and their origin as high temperature condensates, Earth Planet. Sci. Lett. 23, 1–7, 1974.
2 B. Mason and S.R. Taylor, Inclusions in the Allende meteorite, Smithsonian Contrib. Earth Sci. 25, 1982.
3 H. Palme and F. Wlotzka, A metal particle from a Ca,Al-rich inclusion from the meteorite Allende, and the condensation of refractory siderophile elements, Earth Planet. Sci. Lett. 33, 45–60, 1976.
4 A. El Goresy, K. Nagel and P. Ramdohr, Fremdlinge and their noble relatives, Proc. 9th Lunar Planet. Sci. Conf., pp. 1279–1303, 1978.
5 B. Mason and P.M. Martin, Geochemical differences among components of the Allende meteorite, Smithsonian Contrib. Earth Sci. 19, 84–95, 1977.
6 W.V. Boynton, Fractionation in the solar nebula: condensation of yttrium and the rare earth elements, Geochim. Cosmochim. Acta 39, 569–584, 1975.
7 L. Grossman, Refractory trace elements in Ca-Al-rich inclusions in the Allende meteorite, Geochim. Cosmochim. Acta 37, 1119–1140, 1973.
8 E. Stolper, Crystallization sequences of Ca-Al-rich inclusions from Allende: an experimental study, Geochim. Cosmochim. Acta 46, 2159–2180, 1982.
9 J.A. Wood, The interstellar dust as a precursor of Ca,Al-rich inclusions in carbonaceous chondrites, Earth Planet. Sci. Lett. 56, 32–44, 1981.
10 R.E. Cohen, A.S. Kornacki and J.A. Wood, Mineralogy and petrology of chondrules and inclusions in the Mokoia CV3 chondrite, Geochim. Cosmochim. Acta 47, 1731–1757, 1983.
11 A.S. Kornacki and R.E. Cohen, The origin of fine- to medium-grained CAI's in the Allende C3(V) chondrite, Harvard-Smithsonian Center for Astrophys., Preprint No. 1617, 1982.
12 A.G.W. Cameron and M.B. Fegley, Nucleation and condensation in the primitive solar nebula, Icarus 52, 1–13, 1982.
13 L. Grossman and R. Ganapathy, Trace elements in the Allende meteorite, II. Fine-grained, Ca-rich inclusions, Geochim. Cosmochim. Acta 40, 967–977, 1976.
14 J.D. Macdougall, Refractory-element-rich inclusions in CM meteorites, Earth Planet. Sci. Lett. 42, 1–6, 1979.
15 G.J. MacPherson, M. Bar-Matthews, T. Tanaka, E. Olsen and L. Grossman, Refractory inclusions in the Murchison meteorite, Geochim. Cosmochim. Acta 47, 823–839, 1983.
16 T. Tanaka, A.M. Davis, I.D. Hutcheon, M. Bar Matthews, E. Olsen, G.J. MacPherson and L. Grossman, Refractory inclusions in Murchison: chemistry and Mg isotopic composition, Lunar Planet. Sci. XI, 1122–1124, 1980.
17 H. Palme, F. Wlotzka, K. Nagel and A. El Goresy, An ultra-refractory inclusion from the Ornans carbonaceous chondrite, Earth Planet. Sci. Lett. 61, 1–11, 1982.
18 I. Kawabe, L. Grossman, T. Tanaka and A.M. Davis, Trace elements in refractory inclusions from the Murchison C2 chondrite, Meteoritics 16, 338–339, 1981.
19 W.V. Boynton, R.M. Frazier and J.D. Macdougall, Identification of an ultra-refractory component in the Murchison meteorite, Lunar Planet. Sci. XI, 103–105, 1980.
20 A. El Goresy, H. Palme, H. Yabuki, K. Nagel and P. Ramdohr, A refractory inclusion from the Essebi (CM2) carbonaceous chondrite, Lunar Planet. Sci. XIV, 173–174, 1983.
21 L. Grossman and R. Ganapathy, Trace elements in the Allende meteorite, I. Coarse-grained, Ca-rich inclusions, Geochim. Cosmochim. Acta 40, 331–344, 1976.
22 J.M. Allen, L. Grossman, A.M. Davis and I.D. Hutcheon, Mineralogy, textures and mode of formation of a hibonite-bearing Allende inclusion, Proc. 9th Lunar Planet. Sci. Conf., pp. 1209–1233, 1978.
23 J.F. Lovering, D.A. Wark and D.K.B. Sewell, Refractory oxide, titanate, niobate and silicate accessory mineralogy of some Type B Ca-Al-rich inclusions in the Allende meteorite, Lunar Planet. Sci. X, 745–747, 1979.
24 A. El Goresy, K. Nagel and P. Ramdohr, Spinel framboids and fremdlinge in Allende inclusions: possible sequential markers in the early history of the solar system, Proc. 10th Lunar Planet. Sci. Conf., pp. 833–850, 1979.
25 L.H. Fuchs and M. Blander, Refractory metal particles in refractory inclusions in the Allende meteorite, Proc. 11th Lunar Planet. Sci. Conf., pp. 929–944, 1980.
26 D.A. Wark and J.F. Lovering, Refractory/platinum metals and other opaque phases in Allende Ca-Al-rich inclusions (CAI's), Lunar Planet. Sci. IX, 1214–1216, 1978.
27 H. Nagasawa, D.P. Blanchard, J.W. Jacobs, J.C. Brannon, J.A. Philpotts and N. Onuma, Trace element distribution in

mineral separates of the Allende inclusions and their genetic implications, Geochim. Cosmochim. Acta 41, 1587–1600, 1977.

28 L. Grossman, R. Ganapathy and A.M. Davis, Trace elements in the Allende meteorite, III. Coarse-grained inclusions revisited, Geochim. Cosmochim. Acta 41, 1647–1664, 1977.

29 D.A. Wark and G.J. Wasserburg, Anomalous mineral chemistry of Allende FUN inclusions C1, EK-141 and EGG-3, Lunar Planet. Sci. XI, 1214–1216, 1980.

30 B. Fegley, Jr. and A.S. Kornacki, The geochemical behavior of refractory noble metals and lithophile trace elements in CAI's, Lunar Planet. Sci. XIV, 187–188, 1983.

31 A.F. Noonan, J. Nelen, K. Fredriksson and D. Newbury, Zr-Y oxides and high-alkali glass in an amoeboid inclusion from Ornans, Meteoritics 12, 332–335, 1977.

32 L. Brewer and P.R. Wengert, Transition metal alloys of extraordinary stability; an example of generalized Lewis-acid-base interactions in metallic systems, Metall. Trans. 4, 83–104, 1973.

33 J.H. Jones and D.S. Burnett, Laboratory studies of actinide metal-silicate fractionation, Proc. 11th Lunar Planet. Sci. Conf., pp. 995–1001, 1980.

34 JANAF Thermochemical Tables, 2nd ed., No. NSRDS-NBS-37, D.R. Stull and H. Prophet, eds., U.S. Government Printing Office, Washington, D.C., 1971.

35 O. Kubaschewski and C.B. Alcock, Metallurgical Thermochemistry, 5th ed., Pergamon Press, Oxford, 1979.

36 R. Ganapathy and L. Grossman, The case for an unfractionated $^{244}Pu/^{238}U$ ratio in high-temperature condensates, Earth Planet. Sci. Lett. 31, 386–392, 1976.

37 W.V. Boynton, Fractionation in the solar nebula, II. Condensation of Th, U, Pu, and Cm, Earth Planet. Sci. Lett. 40, 63–70, 1978.

38 E.A. King, Refractory residues, condensates and chondrules from solar furnace experiments, Proc. 13th Lunar Planet. Sci. Conf., J. Geophys. Res. 87, A429–A434, 1982.

39 A.S. Kornacki and B. Fegley, Jr., Origin of spinel-rich chondrules and inclusions in carbonaceous and ordinary chondrites, Proc. 14th Lunar Planet. Sci. Conf. (in press).

40 M.B. Fegley, Hibonite condensation in the solar nebula, Lunar Planet. Sci. XIII, 211–212, 1982.

41 D.A. Wark and J.F. Lovering, Evolution of Ca-Al-rich bodies in the earliest solar system: growth by incorporation, Geochim. Cosmochim. Acta 46, 2595–2607, 1982.

42 S. Jovanovic and G.W. Reed, Jr., Noble metal sites in Allende—chemical evidence, Meteoritics 16, 334–335, 1981.

43 E. Anders and M. Ebihara, Solar-system abundances of the elements, Geochim. Cosmochim. Acta 46, 2363–2380, 1982.

44 L.J. Cabri, ed., Platinum-Group Elements: Mineralogy, Geology, Recovery, Can. Inst. Min. Metall., Spec. Vol. 23, 267 pp., Harpell's Press, Quebec, 1981.

45 E. Anders, R. Hayatsu and M.H. Studier, Organic compounds in meteorites, Science 182, 781–790, 1983.

46 E.B. Watson and T.M. Harrison, Zircon saturation revisited: temperature and composition effects in a variety of crustal magma types, Earth Planet. Sci. Lett. 64, 295–304, 1983.

47 R.H. Rein and J. Chipman, Activities in the liquid solution SiO_2-CaO-MgO-Al_2O_3 at 1600°C, Trans. AIME 233, 415–425, 1965.

48 D.A. Wark, Birth of the presolar nebula: the sequence of condensation revealed in the Allende meteorite, Astrophys. Space Sci. 65, 275–295, 1979.

49 B. Fegley, The stability of refractory noble metal-transition metal alloys in enstatite chondrites and aubrites, paper presented at the 46th Annual Meteoritical Society Meeting, Mainz, September 5–9, 1983.

50 P.J. Meschter and W.L. Worrell, An investigation of high temperature thermodynamic properties in the Pt-Zr and Pt-Hf systems, Metall. Trans. 8A, 503–509, 1977.

51 A.M. Davis, T. Tanaka, L. Grossman, T. Lee and G.J. Wasserburg, Chemical composition of HAL, an isotopically-unusual Allende inclusion, Geochim. Cosmochim. Acta 46, 1627–1651, 1982.

52 E. Stolper and P. Ihinger, The color of meteoritic hibonite: an indicator of oxygen fugacity, Lunar Planet. Sci. XIV, 749–750, 1983.

53 M.F. Yan and W.W. Rhodes, Effects of cation contaminants in conductive TiO_2 ceramics, J. Appl. Phys. 53, 8809–8818, 1982.

54 H.M. O'Bryan and M.F. Yan, Second-phase development in Ba-doped rutile, J. Am. Ceram. Soc. 65, 615–619, 1982.

55 D.D. Clayton, Precondensed matter: key to the early solar system, Moon Planets 19, 109–137, 1978.

56 B.M.P. Trivedi and J.W. Larimer, A semiempirical model for heavy element depletion in the interstellar medium, Astrophys. J. 248, 563–568, 1981.

57 D.A. Wark, Evidence for Fe-Ni-S dust fractionation in the protosolar nebula, Lunar Planet. Sci. XIV, 824–825, 1983.

58 E.B. Norman and D.N. Schramm, ^{182}Hf chronometer for the early solar system, Nature 304, 515–516, 1983.